



Probing the B- & C-rings of the antimalarial tetrahydro- β -carboline MMV008138 for steric and conformational constraints

Sha Ding^a, Maryam Ghavami^a, Joshua H. Butler^b, Emilio F. Merino^b, Carla Slebodnick^a, Maria B. Cassera^b, Paul R. Carlier^{a,*}

^a Department of Chemistry and Virginia Tech Center for Drug Discovery, Virginia Tech, Blacksburg, VA 24061, United States

^b Department of Biochemistry and Molecular Biology and Center for Tropical and Emerging Global Diseases (CTEGD), University of Georgia, 120 Green Street, Athens, GA 30602, United States

ARTICLE INFO

Keywords:

Malaria
Plasmodium
MEP pathway
PfIspD

ABSTRACT

The antimalarial candidate MMV008138 (**1a**) is of particular interest because its target enzyme (IspD) is absent in human. To achieve higher potency, and to probe for steric demand, a series of analogs of **1a** were prepared that featured methyl-substitution of the B- and C-rings, as well as ring-chain transformations. X-ray crystallography, NMR spectroscopy and calculation were used to study the effects of these modifications on the conformation of the C-ring and orientation of the D-ring. Unfortunately, all the B- and C-ring analogs explored lost *in vitro* antimalarial activity. The possible role of steric effects and conformational changes on target engagement are discussed.

Malaria was estimated to be responsible for 405,000 deaths worldwide in 2018.¹ Many prevention methods and drug treatment protocols are available, but emerging resistance to artemisinin and its partner drugs is of great concern. Thus there is a pressing need to develop antimalarials that possess new mechanisms of action.² Malaria is caused by *Plasmodium* parasites, of which *P. falciparum* is the most prevalent, accounting for > 96% of the malaria cases worldwide.¹ *Plasmodium* sp. contain a relict organelle termed the apicoplast, which is responsible for the biosynthesis of the critical isoprenoid precursors isopentenyl diphosphate (IPP) and dimethylallyl diphosphate (DMAPP).³ Whereas *Plasmodium* sp. synthesize these compounds via the methylerythritol phosphate (MEP) pathway, the mevalonate pathway is used to synthesize them in humans.³ This biochemical divergence commends the MEP pathway as a target for antimalarial drug development,⁴ since inhibitors of MEP target enzymes would not adversely affect IPP biosynthesis in humans.

Our initial work in this area⁵ identified MMV008138 as a MEP pathway inhibitor, by performing a phenotypic screen of the 400-compound Malaria Box⁶ with the IPP rescue protocol.³ MMV008138 is a tetrahydro- β -carboline, and differentially-functionalized examples of this scaffold are found in a number of other antimalarials,⁷ and compounds directed towards other indications.⁸ Subsequent resistance

selection studies by Wu et al. demonstrated that 2-C-methyl-D-erythritol-4-phosphate cytidyltransferase (IspD, E.C.2.7.7.60), the third enzyme in the MEP pathway, is the target of MMV008138.⁹ Initially, the absolute configuration of MMV008138 was unknown, since it was not disclosed in the Malaria Box; subsequently three independent investigations^{9–11} demonstrated that the active stereoisomer is (1R,3S)-configured, as depicted in **1a** in Fig. 1. Kinetic studies established that **1a** competes with cytidine triphosphate (CTP) in its IspD-catalyzed reaction with 2-C-methyl-D-erythritol-4-phosphate.¹¹

A collection of D-ring analogs of **1a** was prepared by the Pictet-Spengler (PS) reaction of L-Trp-OMe-HCl with various benzaldehydes, separation of diastereomers, and hydrolysis.¹⁰ Examination of these analogs in both *in vitro* growth inhibition (SYBR Green) and *P. falciparum* IspD (PfIspD) inhibition assays show a very close correlation between growth inhibition (EC₅₀) and target engagement (IC₅₀).^{10b} These data also demonstrate a very tight SAR on the D-ring. At least one halogen is required on the 2'- or 4'- position to retain potency in both assays, as shown in Fig. 1; substitution at other D-ring positions is not tolerated. It thus appears that the D-ring of **1a** binds within a snug, well-defined pocket of PfIspD. In the absence of an X-ray structure for this species of IspD,¹² we have speculated^{10b} that halogen-bonding¹³ contributes to the affinity of **1a** for its target.

Abbreviations: PS, Pictet-Spengler; MEP, methylerythritol phosphate; IPP, isopentenyl diphosphate; DMAPP, dimethylallyl diphosphate; Pf, *Plasmodium falciparum*; RMSD, root-mean-square deviation

* Corresponding author.

E-mail address: pcarlier@vt.edu (P.R. Carlier).

<https://doi.org/10.1016/j.bmcl.2020.127520>

Received 1 June 2020; Accepted 22 August 2020

Available online 06 September 2020

0960-894X/© 2020 Elsevier Ltd. All rights reserved.

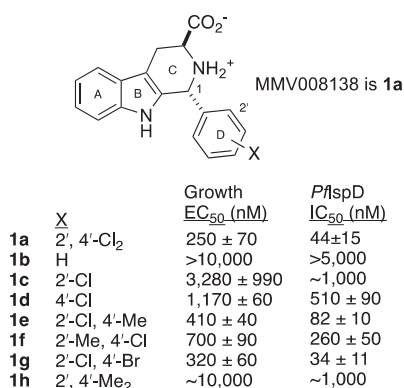
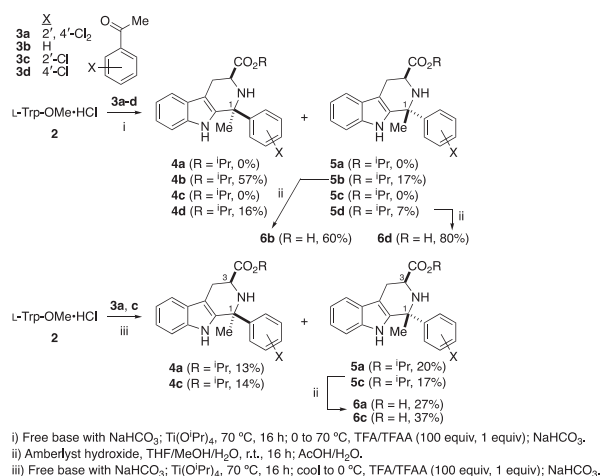


Fig. 1. Lead compound **1a** and tight D-ring SAR. Note that the X = 2'-Br, 4'-Cl and X = 2'-Cl, 4'-F analogs are also potent in both assays.¹⁰



Scheme 1. Synthesis of C1-Me analogs of **1a**.

Since the *in vitro* potency of **1a** was not improved by modulation of the D-ring, we sought to probe the steric requirements for binding around the B- and C-rings, in the hope of identifying more potent analogs. Previously we disclosed analogs **6b** and **6d** (Scheme 1),^{10b} which feature methyl substitution at C1, but with non-optimal substitution of the D-ring (X = H (**6b**), X = 4'-Cl (**6d**)). We attributed the low growth inhibition potency of these compounds to the absence of 2',4'-dichloro substitution. Synthesis of such C1-Me analogs of **1a** requires PS reaction of L-Trp-OMe·HCl **2** with acetophenones **3**, which are significantly less electrophilic than benzaldehydes. Thus, the ester precursors to **6b** and **6d** were prepared by PS reaction with acetophenones **3b** and **3d**, according to Horiguchi's protocol:¹⁴ ketimine formation in neat Ti(OⁱPr)₄, followed by treatment with TFA and TFAA, all at 70 °C. As we noted in our earlier publication,^{10b} application of the Horiguchi protocol to *ortho*-substituted acetophenones **3a** and **3c** did not give the expected products. However, we subsequently found that if ketimine formation was followed by treatment with TFA/TFAA at 0 °C to room temperature, the desired *trans*-esters **5a** and **5c** could be isolated in 20% and 17% yield respectively (isopropyl esters result from Ti(OⁱPr)₄-mediated transesterification). As detailed by Horiguchi,¹⁴ the *trans*-relative configuration of **5a** and **5c** was established by the absence of an NOE correlation between H3 and the C1-methyl; this correlation is visible in the corresponding *cis*-isomers **4a** and **4c** (Supplementary Material, Figs. S2–S3). Hydrolysis of **5a** and **5c** afforded the desired amino acids **6a** and **6c**.

Unfortunately, the presence of a 2'-Cl substituent in the D-ring of these C1-methyl analogs did not restore antimalarial activity (Table 1, entries 6, 8). Compared to our lead **1a** (EC₅₀ = 250 ± 70 nM), C1-methyl analog **6a** shows no growth inhibition at 10,000 nM. Similarly,

Table 1

P. falciparum growth inhibition by **1a–d**, **f**, and indicated B- and C-ring analogs.

Entry	Compound	Dd2 strain <i>P. falciparum</i> Growth EC ₅₀ (nM)
1	1a	250 ± 70 ^{a,c}
2	1b	> 10,000 ^a
3	1c	3280 ± 990 ^{a,d}
4	1d	1170 ± 60 ^{a,e}
5	1f	700 ± 90 ^{a,c}
6	6a	> 10,000
7	6b	> 10,000 ^b
8	6c	> 10,000
9	6d	> 10,000 ^b
10	8a	190 ± 30 ^a
11	12f	> 10,000
12	12i	> 10,000
13	16a	65% inhibition at 10 μM
14	(±)- 20a	> 10,000
15	24a	~8000
16	25a	> 10,000
17	26a	> 10,000

^aReported previously.^{10a} ^bReported previously.^{10b} ^c100% rescued by 200 μM IPP @ 10 μM. ^d60% rescued by 200 μM IPP @ 10 μM. ^e50% rescued by 200 μM IPP @ 10 μM. ^f100% rescued by 200 μM IPP @ 2.5 μM.

the weakly potent 2'-Cl substituted **1c** (EC₅₀ = 3280 ± 990 nM) loses all growth inhibition potency upon C1-methylation (**6c**, no growth inhibition at 10,000 nM). Since the mere addition of a methyl group at C1 should not drastically affect permeability or transport of these compounds, we conclude that the loss of growth inhibition potency is due to reduced affinity for PflspD, the target of **1a** (and its potent analogs, cf. Fig. 1). In particular, it appears that either there is no room in the PflspD binding pocket for a methyl group at C1, or that the C1-methyl in **6a** induces a conformational change that disfavors binding. We were fortunate to obtain a crystal of **7a** (Fig. 2), the methyl amide derivative of **6a**, and to compare it to **8a**, the methyl amide analog of **1a**, which we previously crystallized.^{10a} Since **8a** is equipotent (Dd2 strain growth EC₅₀ = 190 ± 30 nM) with **1a**, comparison of the conformations of **7a** and **8a** could be informative.

As can be seen in Fig. 2, the tetrahydropyridine C-rings of **7a** and **8a** adopt very similar conformations, featuring a pseudoequatorial C(O)NHMe group and an apparent electrostatic interaction between the amide NH and the tetrahydropyridine nitrogen N2 (Fig. 2). There are 4 molecules of **7a** in the unit cell, and the average RMSD of the 6C-ring atoms of them from **8a** is 0.041 Å (individual values 0.030, 0.033, 0.046, 0.057 respectively). However, steric strain between the C1-Me and the C2'-Cl in **7a** causes the D-ring to adopt a different orientation. We define τ as the dihedral angle between the C1 substituent (CH₃ for **7a**, H for **8a**), C1, C1', and C2'. For **7a** (C1-Me), the average τ value is −63.6° (individual values −59.15°, −62.29°, −64.00°, and −68.91°, respectively), whereas the τ value in **8a** (C1-H) is nearly 30° smaller, at −36.5°.

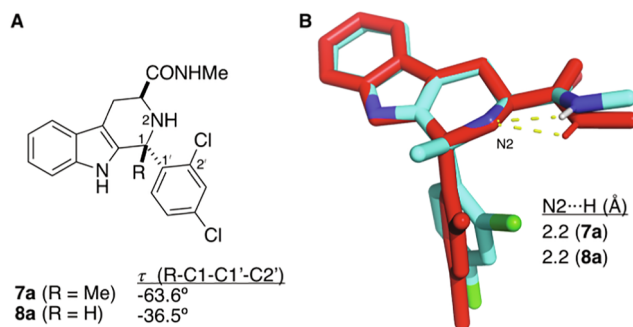
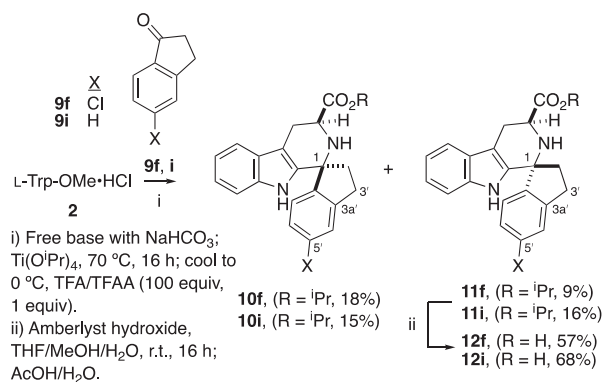
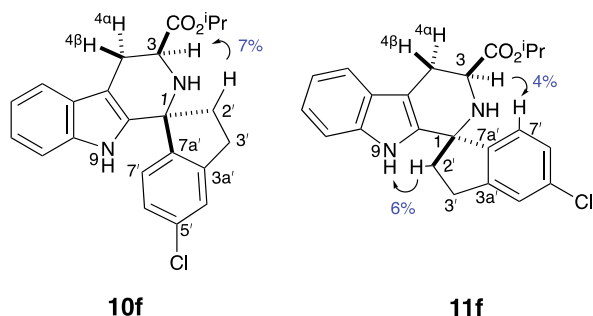
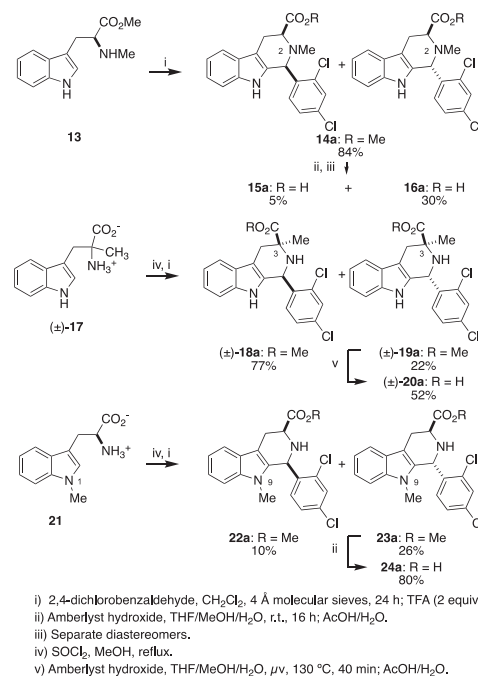


Fig. 2. A. Comparison of τ (R-C1-C1'-C2') dihedral angles in **7a** and **8a**. B) PyMOL¹⁵ overlay of X-ray structures of **7a** (cyan; carbon; blue: nitrogen; green: chlorine) and **8a** (red). A thermal ellipsoid depiction of **7a** is provided in the Supporting Information, Fig. S1).

Scheme 2. Synthesis of spirofused analogs **12f**, **12i**.

Given the extreme sensitivity of growth and *Pfl*spD inhibition to substitution of the D-ring (see Table 1), it is possible that this dihedral angle change alone, apart from the added steric bulk at C1, could be deleterious to potency. To enforce a smaller τ dihedral angle, we thus proposed to connect C1 and C2' with an ethylene bridge as shown in **12f** and **12i** (Scheme 2), imparting a cipargamin^{7b}-like spirofusion. Compound **12f** would thus be a conformationally-constrained mimic of 2'-Me,4'-Cl-substituted **1f**, which has significant potency (EC₅₀ = 700 ± 90 nM). The ketone PS reaction between L-Trp-OMe·HCl **2** and indanones **9f/9i** was performed according to the original Horiguchi protocol;¹⁴ diastereomer separation gave esters **11f** and **11i**, which mimic the *trans*-orientation of **5a-d**. The *trans*-configuration of **11f** and *cis*-configuration of **10f** was confirmed via 1D NOE experiments (Fig. 3).

Irradiating C3-H revealed NOE to C7'-H for the *trans*-isomer **11f**, but not for the *cis*-isomer **10f**. When one of the diastereotopic C2'-H is irradiated in **11f**, NOE to the N9-H is seen. In contrast, irradiation of one of the diastereotopic C2'-H in the *cis*-isomer **10f** transfers NOE to C3-H (Supplementary Material, Figs. S4–S7). Interestingly, ¹H NMR analysis of **11f**, **11i** and their *cis*-diastereomers (**10f**, **10i**) demonstrated one large and one small coupling constant of H3 to the H4 protons, indicating a near antiperiplanar relationship of H3 and H4 β . Thus, regardless of *cis*- or *trans*-orientation, the 3-CO₂ⁱPr group is pseudoequatorial, and H3 is pseudoaxial. The *trans*-esters **11f** and **11i** were then hydrolyzed to give the desired spirofused analogs **12f** and **12i**. Unfortunately, neither compound was potent for growth inhibition (Table 1, entries 11–12). Compound **12f** (EC₅₀ > 10,000 nM) differs from **1f** (EC₅₀ = 700 ± 90 nM) by substitution of the C2'-CH₃ group with an ethylene bridge to C1. Molecular mechanics-based conformational analysis^{16,17} of the methyl amide of **11f** (**11f** NHMe), demonstrates that the spiroring fusion generates two conformer ensembles defined by narrow ranges in the τ dihedral angle (here C2'-C1-C7a'-C3a', Fig. 3). One ensemble (13 conformers) features τ = -19 ± 1°, more similar to that of **8a** (τ = -36.5°) than of **7a** (τ = -63.8°). The other ensemble (16 conformers) features τ = +17 ± 2°. Since the lowest energy conformers in each ensemble are similar in energy

Fig. 3. 1D NOE observed in **10f** and **11f**.Scheme 3. Synthesis of **16a**, (±)-**20a**, and **24a**.

(Supplementary Material, Table S1), both conformers are expected to be populated, and be available to bind *Pfl*spD. Thus, unless the τ dihedral angle exhibited by **8a** (and presumably **1a**) precisely matches the steric requirement of *Pfl*spD, it seems most likely that the low potency of spirofused analog **12f**, is due to steric bulk at the C1 position, as we concluded for C1-Me analogs **6a** and **6c**.

To probe the effect of substitution at other positions, we prepared analogs featuring methylation at N2, C3, and N9 (Scheme 3). Since we have shown that antimalarial potency of **1a** and analogs requires *trans*-(1R,3S)-configuration,¹⁰ we took special pains to ensure that we had isolated the correct stereoisomer in each case. The N2-Me analog **16a** was prepared from PS reaction of N α -methyl-L-tryptophan methyl ester **13** and 2,4-dichlorobenzaldehyde **3a**. The PS adduct **14a** was isolated as an inseparable mixture of diastereomeric methyl esters, hydrolyzed, and separated by reverse phase prep-HPLC into the *cis*-isomer **15a** and the *trans*-isomer **16a**. The relative configuration of these isomers was assigned on the basis of the H3-H4 α and H3-H4 β coupling constants (³J_{34 α} and ³J_{34 β}). As Van Linn et al. have shown for 1,2,3-trisubstituted PS adducts, 1,3-*trans*-configured compounds have ³J_{34 α} ≈ ³J_{34 β} = 4.4–4.9 Hz.¹⁸ In contrast, 1,3-*cis*-configured-1,2,3-trisubstituted PS adducts have differentiated values for these coupling constants (³J_{34 α} = 3.8–5.2 Hz and ³J_{34 β} = 6.5–8.0 Hz).

The racemic C3-Me analog (±)-**20a** was prepared from α -methyl-DL-tryptophan (±)-**17**. Esterification with SOCl₂/MeOH followed by PS reaction with 2,4-dichlorobenzaldehyde **3a** gave *cis*-ester (±)-**18a** and *trans*-ester (±)-**19a**; the relative configuration of these compounds was established by 1D NOE experiments (Fig. 4). Irradiating the C3-Me in (±)-**18a** shows NOE to H1, but no such NOE is seen on irradiation of the C3-Me in (±)-**19a**. In addition, irradiation of the C3-Me in (±)-**18a** shows NOE signal to H4 α , but not H4 β . In contrast, irradiation of the C3-Me in (±)-**19a** shows NOE to both H4 α and H4 β (Supplementary Material, Figs. S8–S9). Hydrolysis of the *trans*-ester (±)-**19a** was again accomplished with the catch and release protocol,¹⁹ but required elevated temperature, possibly due to steric hindrance caused by the C3-Me.

The N9-Me analog **24a** was prepared by esterification of 1-Me-L-tryptophan **28**, PS reaction with 2,4-dichlorobenzaldehyde **3a**, separation of diastereomers **22a** and **23a**, and hydrolysis of **23a**. (Scheme 3). The relative configuration of the diastereomeric esters **22a** and **23a**

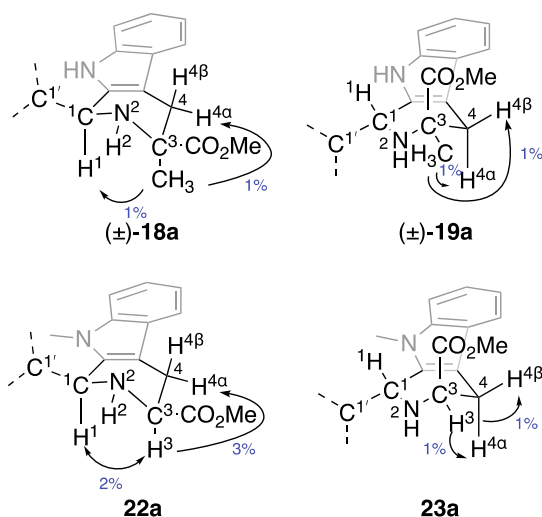
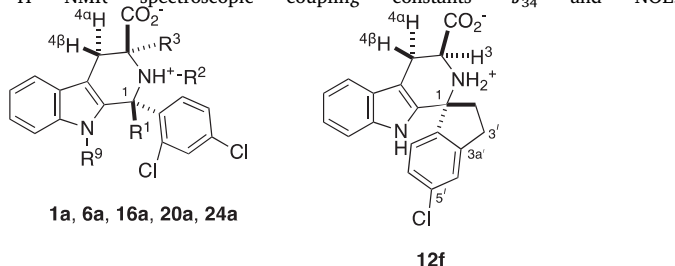


Fig. 4. Assignment of relative configuration in (±)-18a/(±)-19a and 22a/23a by 1D NOE.

Table 2

Predominant orientation of the 3-CO₂[−] group in **1a** and analogs, as judged by ¹H NMR spectroscopic coupling constants ³J₃₄ and NOE.



Entry	Cpd	R ¹	R ²	R ³	R ⁹	³ J ₃₄ ^a (Hz)	3-CO ₂ [−]
1	1a	H	H	H	H	8.5, 5.5	ψ _{eq} & ψ _{ax}
2	6a	CH ₃	H	H	H	12.0, 5.1	ψ _{eq}
3	12f	na	na	na	na	11.7, 5.0	ψ _{eq}
4	24a	H	H	H	CH ₃	10.3, 4.9	ψ _{eq}
5	16a	H	CH ₃	H	H	5.0, 5.0	ψ _{ax}
6	(±)- 20a	H	H	CH ₃	H	NOE ^b	ψ _{ax}

^a ¹H NMR spectra measured in CD₃OD.

^b Predominant conformation determined by ¹H-¹H NOE experiments, since R³ = CH₃, see text.

was again assigned by 1D NOE spectroscopy. Irradiating H3 of the *cis*-isomer **22a** shows an NOE signal to H1, but this correlation is not seen in *trans*-isomer **23a** (Fig. 4). In addition, irradiation of H3 in **23a** shows NOE signals to both H4α and H4β, indicating the 3-CO₂Me group is pseudoaxial orientation. For **22a** a strong correlation of H3 to H4α is observed, as shown in Fig. 4 (Supporting Material, Figs. S11–S12).

As can be seen in Table 1, methyl substitution at N2, C3 and N9 (compounds **16a**, (±)-**20a** and **24a**, respectively) unfortunately abrogates *P. falciparum* growth inhibition (EC₅₀ ≥ 8000 nM, entries 13–15). As we concluded for methylation at C1 (e.g. **6a**, entry 6), we consider it unlikely that addition of a methyl group would significantly impact permeability or transport, and we conclude that these modifications reduce affinity for PfIsPD. Again, steric hindrance to binding caused by methylation at N2, C3 and N9 may be responsible. However, since studies of the stereoisomers^{9–11} and C3-variants¹⁰ of **1a** indicate that interaction of the 3-CO₂[−] group with PfIsPD is important for affinity, we thought it is important to rule out less direct explanations for the low potency of these compounds. In particular, we sought to determine whether substitution at C1, N2, C3, and N9 could strongly bias a pseudoequatorial- (ψ_{eq}) or pseudoaxial- (ψ_{ax}) orientation of the 3-

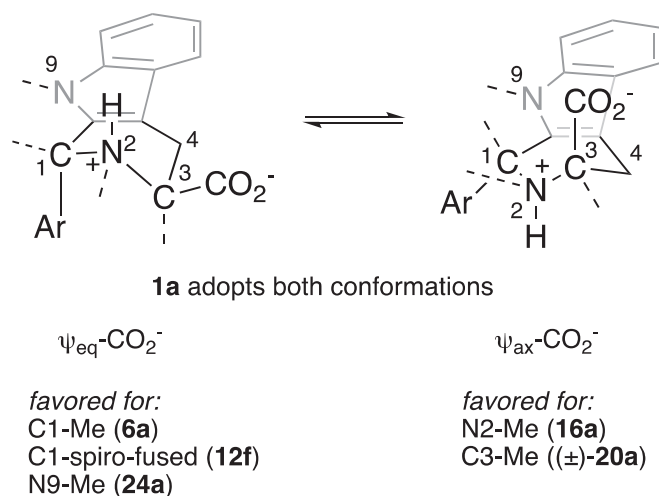
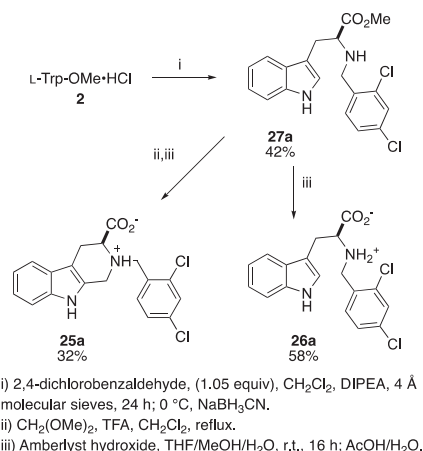


Fig. 5. Effects of C1-, N2, C3- and N9 substitution on the preferred conformation of the tetrahydropyridine C-ring of **1a**.



Scheme 4. Synthesis of shifted and open C-ring analogs of **1a**.

CO₂[−] group in the tetrahydropyridine ring.

Thus, for **1a**, **6a**, **12f**, **16a** and **24a**, we examined ¹H-¹H coupling constants between H3 and H4α, and between H3 and H4β (Table 2). Since (±)-**20a** lacks a proton at C3, we used NOE to deduce the preferred orientation of the 3-CO₂[−] group, as was done for the methyl ester precursor (±)-**19a** (Fig. 4). Due to reasons of solubility, these experiments were carried out in CD₃OD; we do recognize that the conformational thermodynamics could vary somewhat in water. However as described in the supporting information (Supporting Material, Section F), in large part the conformer preferences seen comport with the principles of maximizing ψ_{eq}-substitution, and relief of torsional strain. These effects are summarized in Fig. 5.

Thus, as anticipated, substitution at C1, N2, C3, and N9 does affect the preferred conformations of these analogs of **1a**. However, since neither enforced ψ_{eq}-CO₂[−]-orientation (e.g. **6a**, **12f**, **24a**) nor enforced ψ_{ax}-3-CO₂[−]-orientation (e.g. **16a**, (±)-**20a**) conferred potency, it appears that the low potency of these compounds is indeed steric in origin.

Finally, in addition to installing substituents on the B- and C-rings, we also investigated the shifted C-ring analog **25a** and the open C-ring analog **26a** (Scheme 4). The reductive amination of L-Trp-OMe·HCl **2** with **3a** and sodium cyanoborohydride gives intermediate **27a**. Subsequent treatment of **27a** with dimethoxymethane and TFA followed by hydrolysis affords the shifted C-ring analog **25a**; hydrolysis of **27a** gives open C-ring analog **26a**. Unfortunately, neither **25a** nor **26a** was potent for growth inhibition of *P. falciparum* (Table 1).

To conclude, placement of a methyl group on the B-ring (N9, e.g. **24a**), C-ring (C1: **6a**; N2: **16a**; C3: (±)-**20a**) and installation of a spirofusion between the C- and D-rings (e.g. **12f**) all drastically reduced *in vitro* antimalarial potency. In addition to the obvious consequence of increased steric bulk at these positions, these modifications also affected the preferred ψ_{eq^-} or ψ_{ax^-} orientation of the C3-CO₂⁻ group in the tetrahydropyridine C-ring (Table 2), and the orientation of the D-ring (Fig. 2 and text). Lastly, shifted and open C-ring analogs of **1a** (**25a** and **26a**, respectively) were found to lack *in vitro* activity. These structural modifications of **1a** and **1f** are not expected to significantly impact permeation or transport, since they comprise formal addition of a CH₂ unit (e.g. **6d**, **12f**, **12i**, **16a**, **24a**), isomerization (**25a**), or addition of H₂ (**26a**). We conclude therefore that the loss of *P. falciparum* growth inhibition potency is due to lack of target engagement. In particular, we propose that the binding pocket of PflspD features very close contact with the B- and C-rings of **1a**, as we had proposed earlier for the D-ring.^{10b} Whether this close contact also extends to all positions of the A-ring of **1a**, and whether A-ring modifications could improve potency, work is in progress, and will be reported in due course.

Author contributions

P.R.C., S.D., and M.G. designed analogs of **1a**, and S.D. and M.G. synthesized them. J.H.B., E.F.M., and M.B.C. developed and performed the *in vitro* assays. C.S. performed X-ray crystallography. The manuscript was written through contributions of all authors. All authors have given approval to the final version of the manuscript.

Funding sources

Funding from the National Institute of Allergy and Infectious Disease (AI128362 to P.R.C. and M.B.C.; AI108819 to M.B.C.; T32-AI060546 to J.H.B.) is gratefully acknowledged. X-ray crystallographic work was supported by the National Science Foundation under CHE-1726077.

Declaration of Competing Interest

The authors declare that they have no known competing financial interests or personal relationships that could have appeared to influence the work reported in this paper.

Appendix A. Supplementary data

This information is available free of charge on the Elsevier

Publications website, and includes: synthetic procedures and analytical data for all new compounds; NOE spectra; X-ray crystallographic data for **7a**; MMFF94 conformer distribution of **11f** NHMe; *in vitro* *P. falciparum* growth inhibition assay procedures (PDF). Supplementary data to this article can be found online at <https://doi.org/10.1016/j.bmcl.2020.127520>.

References

- World Malaria Report 2019. The World Health Organization, available at <https://www.who.int/publications-detail/world-malaria-report-2019>, last accessed 5/20/20.
- Wells TNC, van Huijsduijnen RH, Van Voorhis WC. *Nat Rev Drug Discov*. 2015;14:424.
- Yeh E, DeRisi JL. *PLoS Biol*. 2011;9:e1001138.
- Hale I, O'Neill PM, Berry NG, Odom A, Sharma R. *MedChemComm*. 2012;3:418.
- Bowman JD, Merino EF, Brooks CF, Striepen B, Carlier PR, Cassera MB. *Antimicrob Agents Chemother*. 2014;58:811.
- Spangenberg T, Burrows JN, Kowalczyk P, McDonald S, Wells TNC, Willis . *PLoS One*. 2013;8:e62906.
- (a) Gupta L, Srivastava K, Singh S, Puri SK, Chauhan PMS. *Bioorg Med Chem Lett*. 2008;18:3306
(b) Rottmann M, McNamara C, Yeung BKS, et al. *Science*. 2010;329:1175
(c) Davis RA, Duffy S, Avery VM, Camp D, Hooper JNA, Quinn RJ. *Tetrahedron Lett*. 2010;51:583
(d) Beghyn TB, Charton J, Leroux F, et al. *J Med Chem*. 2011;54:3222
(e) Gellis A, Dumètre A, Lanzada G, et al. *Biomed Pharmacother*. 2012;66:339
(f) Sharma B, Kaur S, Legac J, Rosenthal PJ, Kumar V. *Bioorg Med Chem Lett*. 2020;30:126810.
- (a) Laine AE, Lood C, Koskinen AMP. *Molecules*. 2014;19:1544
(b) Daugan A, Grondin P, Ruault C, et al. *J Med Chem*. 2003;46:4533
(c) De Savi C, Bradbury RH, Rabow AA, et al. *J Med Chem*. 2015;58:8128
(d) Singh R, Jaisingh A, Maurya IK, Salunke DB. *Bioorg Med Chem Lett*. 2020;30:126869.
- Wu W, Herrera Z, Ebert D, et al. *Antimicrob Agents Chemother*. 2015;59:356.
- (a) Yao Z-K, Krai PM, Merino EF, et al. *Bioorg Med Chem Lett*. 2015;25:1515
(b) Ghavami M, Merino EF, Yao Z-K, et al. *ACS Infect Dis*. 2018;4:549.
- Imlay LS, Armstrong CM, Masters MC, et al. *Infect. Dis*. 2015;1:157.
- Note that several species of IspD (including *Escherichia coli* and *Arabidopsis thaliana*) have yielded high resolution X-ray structures. However, PflspD features several long and apparently unstructured insertions not present in such crystallized IspDs, and **1a** does not potentially inhibit any of these enzymes (ref. 9). Therefore, we do not consider it prudent to carry out docking studies of the compounds described in this paper with PflspD homology models based on these crystallized IspDs.
- Scholfield MR, Zanden CMV, Carter M, Ho PS. *Protein Sci*. 2013;22:139.
- Horiguchi Y, Nakamura M, Saitoh T, Sano T. *Chem Pharm Bull*. 2003;51:1368.
- The PyMOL Molecular Graphics System, Version 1.2r3pre, Schrödinger, LLC.
- (a) Shao Y, Molnar LF, Jung Y, et al. *PCCP*. 2006;8:3172
(b) Halgren TA. *J Comput Chem*. 1996;17:490.
- Spartan'18; Wavefunction, Inc., Irvine, CA, 2014.
- Van Linn ML, Cook JM. *J Org Chem*. 2010;75:3587.
- Morwick TM. *J Comb Chem*. 2006;8:649.